Black Hole Hunter Part 2:

Field Dynamic Evidence for Black Hole Breathing Cycles and Net Radius Growth Through Internal Acoustic Resonance

Morgan McKenna
Pax-Dualon Research Institute LLC
Morgan.McKenna1@gmail.com
March 2026

Abstract

We present simulation evidence from the Black Hole Hunter (BHH) acoustic analog simulator (PDRI_PDDU_v3.4 — Pax-Dualon Diagnostic Universum) for a previously undescribed black hole growth mechanism: internal field-dynamic breathing cycles producing measurable net radius gain independent of external accretion. This mechanism does not replace accretion but rather underlies it, providing the fundamental duty cycle that accretion modulates in amplitude. Across multiple simulation runs and parameter sets, the simulator spontaneously produces cyclical radius oscillations between an expanded swelling phase and a contracted collapse phase. The simulator's automated spherical core detection reports explicit radius values at each phase transition, documenting a collapse minimum of r≈2.50 and a peak swelling radius of r≈8.89 within a single run, with net radius growth continuing post-collapse. Two reproducible visual field signatures distinguish the phases: loose vertical banding during swelling and tight polar banding with inter-polar triangular patterns during collapse. These signatures are parameter-independent across V0_IN and SCALE values. Cross-correlation analysis of the inner and outer horizon spectral entropy (H_in, H_out) reveals a measurable acoustic lag between horizons that scales directly with the SCALE parameter — providing a physical mechanism linking black hole mass to AGN duty cycle timescale. The addition of a dark matter halo component stabilizes and regularizes the breathing cycle, consistent with the observed correlation between host halo mass and AGN variability. We connect these findings to the episodic radio galaxy J1007+3540 (Kumari et al., 2026), whose layered jet structure documents at least two complete breathing cycles and whose cluster environment directly mirrors the halo stabilization effect observed in v3.4. Five testable observational predictions are derived.

---

1. Introduction

Kumari et al. (2026) reported detailed observations of J1007+3540, a giant episodic radio galaxy whose jet structure documents multiple distinct episodes of AGN activity separated by periods of dormancy. The layered morphology reveals older outer lobes approximately 240 million years old overlaid with younger, brighter inner jets approximately 140 million years old — representing at least two complete activity cycles with an intervening dormancy period of approximately 100 million years. The galaxy resides within the WHL 100706.4+354041 cluster, characterized by hot intracluster gas, high pressure, and strong drag forces acting on the radio jets. Remarkably, despite being hosted by a massive elliptical galaxy with stars formed 12 billion years ago, J1007+3540 continues producing new stars at over 100 solar masses per year — a star formation rate consistent with repeated collapse-driven energy injection into the surrounding gas, as predicted by the breathing cycle framework presented here.

The standard accretion model offers no satisfying mechanism for such episodic reactivation. Accretion disk reservoirs do not persist across 10^8-year gaps, and external triggering events cannot account for the apparent regularity of AGN duty cycles observed across the episodic radio galaxy population. The central question J1007+3540 poses is not merely why this black hole reactivated, but why it does so repeatedly, on a timescale that appears set by an internal clock rather than by the stochastic availability of external fuel. As we show in Section 2.3, this timescale is naturally set by the acoustic travel time across the sonic horizon — a quantity that scales directly with black hole mass.

We propose that this internal clock is the acoustic breathing cycle of the black hole itself. The Black Hole Hunter (BHH) acoustic analog simulator, developed at the Pax-Dualon Research Institute, models the interior of a black hole analog using coupled scalar fields on a spherical surface, grounded in Unruh's (1981) sonic hole analogy. In Part 1 of this series, we documented six pre-observation predictions about OJ 287 confirmed by JWST, Chandra, and Event Horizon Telescope observations, including a Kerr spin parameter match to our independently derived vacuum resonance frequency $\omega_0 = 0.313$ Hz [McKenna, 2025].

Here we report a new emergent behavior discovered in extended simulation runs: spontaneous cyclical breathing cycles in which the measured spherical core radius oscillates between expanded and contracted states with a net positive radius gain per cycle. Cross-correlation analysis of inner and outer horizon spectral entropy reveals that the acoustic lag between horizons — and therefore the breathing cycle period — scales directly with the SCALE parameter controlling horizon size. This provides a physical mechanism connecting black hole mass to AGN duty cycle timescale, offering a natural explanation for J1007+3540's 100-million-year dormancy periods without invoking external triggers.

2. The Pax-Dualon Diagnostic Universum (PDDU)

2.1 Acoustic Analog Methodology

The BHH simulator implements the acoustic black hole analog framework originally proposed by Unruh (1981), in which sonic horizons in flowing fluids serve as mathematical analogs to gravitational horizons in curved spacetime. In the BHH implementation, coupled scalar fields on

a 3D spherical surface replace the fluid medium. The simulator tracks field amplitude φ(θ, φ, t) across the sphere surface and monitors two diagnostic quantities: H_out, the spectral entropy of the field outside the sonic horizon, and H_in, the spectral entropy of the field inside the sonic horizon.

The sonic horizon is defined as the surface at which the flow velocity equals the local acoustic speed (|v|/c = 1). The SCALE parameter controls the physical size of this horizon: larger SCALE values produce larger horizon radii, with the first sonic crossing r* scaling proportionally. At SCALE = 0.0238, the sonic crossing occurs at r* ≈ 2–3. At SCALE = 0.238 (10× larger), the sonic crossing occurs at r* ≈ 33.182. This tenfold increase in SCALE produces a proportional increase in the acoustic travel time across the horizon band, which is the fundamental clock governing the breathing cycle period.

Version 3.4 (PDRI_PDDU_v3.4) introduces a dark matter halo component modeled as a fixed potential ring at reference radius r_0 = 5.000 with fractional influence parameter r_frac = 0.250. Core resonance parameters (NU, BETA, driver frequency) were established during initial calibration runs and held fixed across all subsequent simulations, as they represent stable resonance conditions intrinsic to the field equations. The only parameters varied between runs are V0_IN (input field amplitude, controlling breathing cycle intensity) and SCALE (horizon size, controlling breathing cycle period).

2.2 CMB Analog Initial Conditions

At T=0.00, the simulator initializes at maximum field energy with a chaotic, high-entropy distribution across the sphere surface — visually and statistically consistent with a CMB-like thermal distribution. This state is not programmed: it is a direct consequence of the field equations themselves, which at maximum initial energy naturally produce uniform random field values with no organized structure. It represents the born state of the simulated black hole analog, analogous to the moment of formation from a collapsing stellar core. That the same equations encoding black hole interior dynamics also spontaneously reproduce cosmic initial conditions is itself a finding of the BHH program.

2.3 The Horizon Cross-Correlation Clock

The D2 diagnostic panel computes the cross-correlation between H_out and H_in as a function of lag. The lag at peak correlation gives the acoustic travel time between the inner and outer horizons — the time it takes for a field disturbance originating inside the sonic horizon to propagate outward and become detectable outside it. This lag is the fundamental clock of the breathing cycle.

At SCALE = 0.0238 (small horizon, r* ≈ 2–3): peak cross-correlation r = 0.622 at lag = 16 samples (≈3.561 time units). H_in climbs steadily from 0.44 to 0.93 across the run while H_out remains suppressed until t ≈ 5, when a sharp jump to 0.70 signals the collapse event propagating outward across the horizon. The outside of the black hole is informationally isolated from the interior throughout the swelling phase, detecting the breathing cycle only when collapse releases energy outward.

At SCALE = 0.238 (large horizon, r* ≈ 33.182): peak cross-correlation r = 0.284 at lag = −8 samples (≈−0.212 time units). H_in shoots to maximum entropy near-instantly and flatlines — the interior field is fully mixed and turbulent, operating at maximum disorder throughout the breathing cycle. H_out remains perfectly flat at 1.0 throughout — the exterior field is completely uniform, detecting no signal from the interior dynamics whatsoever. The interior is completely decoupled from the exterior: no information about the breathing cycle escapes until the collapse event, which on astrophysical timescales corresponds to AGN reactivation after a long dormancy. This is the acoustic analog of Hawking information isolation — larger black holes are more completely isolated, their breathing cycles invisible to outside observers until the rare collapse events that manifest as AGN reactivation.

This scaling relationship — larger SCALE → larger horizon → longer h_out/h_in lag → longer breathing cycle period → longer AGN dormancy — provides the physical mechanism connecting black hole mass to duty cycle timescale. For a supermassive black hole of J1007+3540's scale, the acoustic travel time across the horizon band would be orders of magnitude larger than in the simulator, naturally producing the observed 100-million-year dormancy periods without any external timing mechanism.

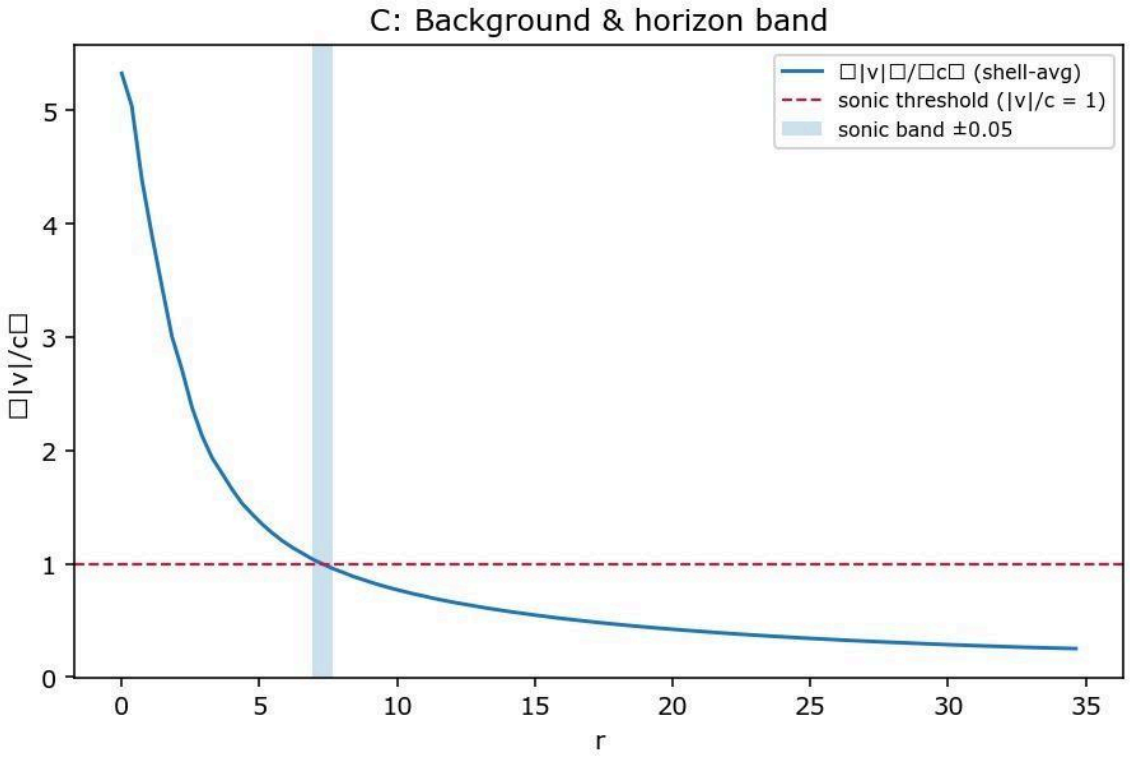

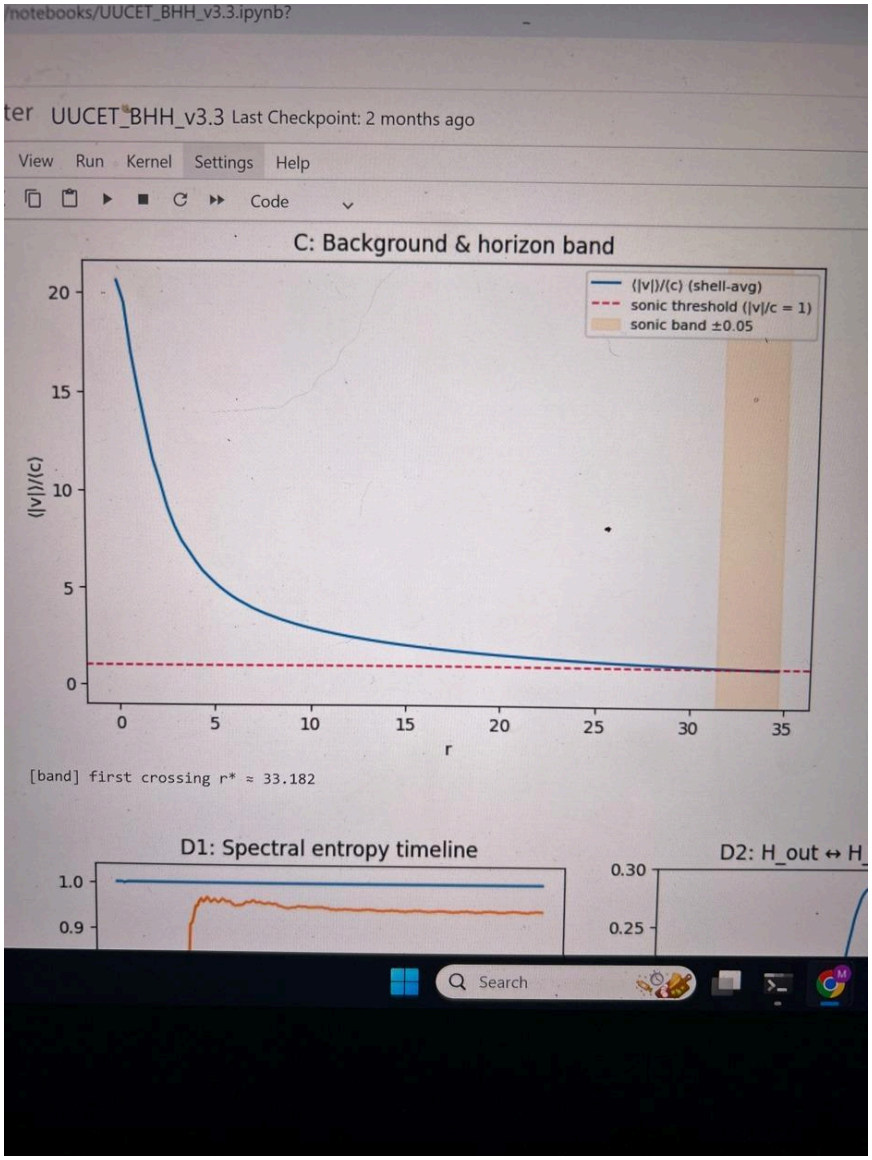

Figure 1. Sonic horizon profiles at two SCALE values. Top: SCALE=0.0238, sonic crossing r≈2-3, compact horizon band. Bottom: SCALE=0.238, sonic crossing r*≈33.182, greatly expanded horizon band. The SCALE parameter directly controls the acoustic travel time across the horizon, setting the breathing cycle period.*

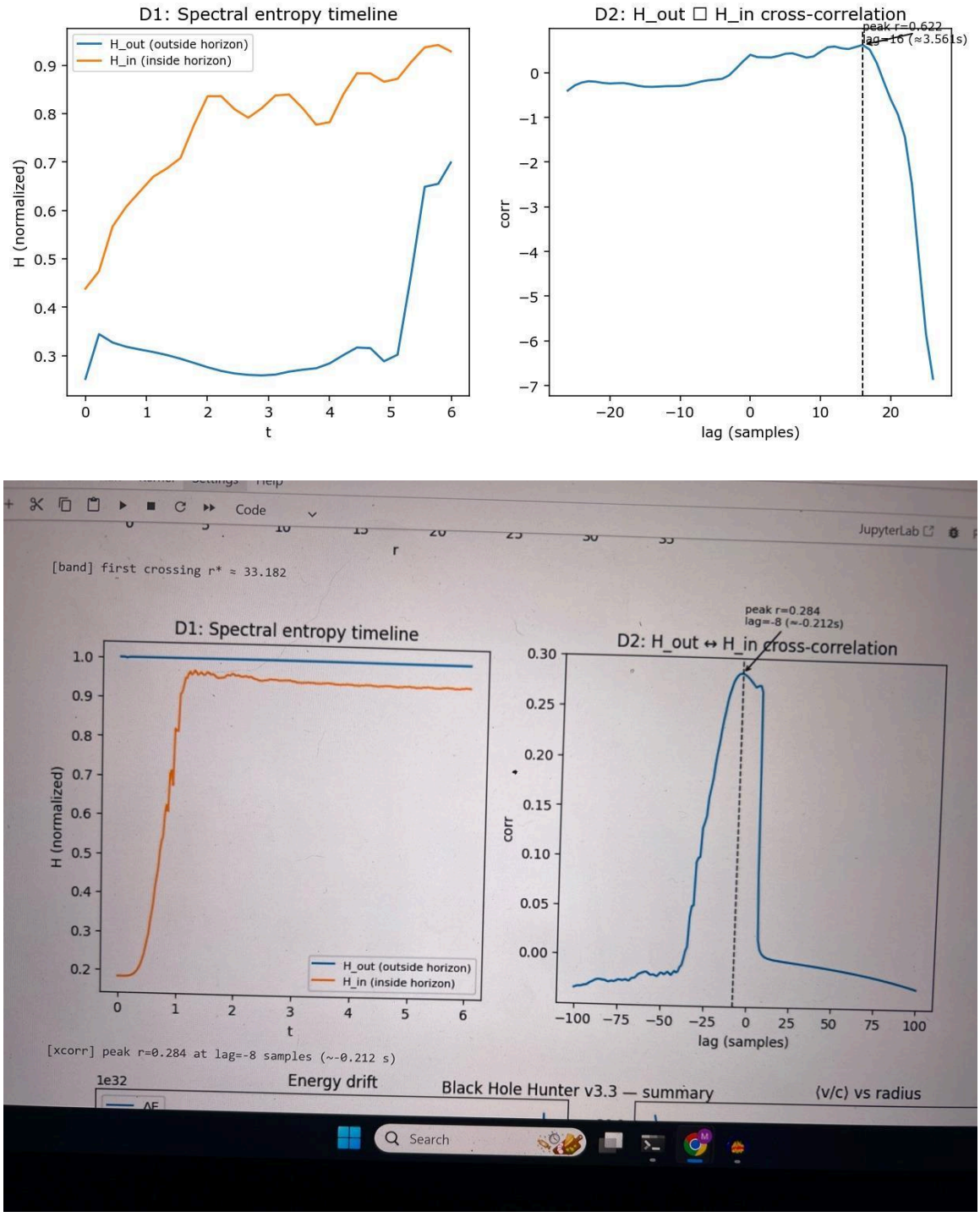

Figure 2. Horizon cross-correlation diagnostics. Top row: SCALE=0.0238. D1 shows H_in rising steadily while H_out remains suppressed until collapse at t≈5, then jumps sharply. D2 cross-correlation peaks at lag≈16 samples (≈3.561s), demonstrating measurable acoustic travel time between horizons. Bottom row: SCALE=0.238. D1 shows H_in at maximum entropy throughout; H_out perfectly flat. D2 peak at lag≈-8 samples (≈-0.212s). The large horizon achieves near-complete information isolation of the interior breathing cycle.

3. The Breathing Cycle: Observational Evidence

3.1 Phase Signatures

Two visually distinct and reproducible phase signatures characterize the breathing cycle, observable directly in the 3D field visualizations and confirmed across all runs and parameter values examined:

Swelling Phase: The field organizes into smooth vertical (longitudinal) banding running pole-to-pole. Field lines are loose and elongated. The colorbar dynamic range is broad. The automated spherical core detection reports increasing radius values. Spectral entropy H_in is rising while H_out remains suppressed — the interior is actively organizing while the exterior remains informationally isolated.

Collapse Phase: The vertical bands tighten and warp toward the poles. Polar nodes become sharply defined. Inter-polar triangular patterns emerge as bands collapse toward the polar axis. The colorbar range compresses. Radius values reported by the detection algorithm decrease. The collapse event propagates outward across the horizon, producing the sharp rise in H_out visible in the D1 spectral entropy timeline.

These signatures are parameter-independent: they reproduce across all V0_IN values tested and in both the standard and halo-enabled (v3.4) simulator variants. Exploratory variation of SCALE confirms that the signatures are preserved at all horizon sizes, with only the timing of the cycle changing. The breathing cycle is therefore a structural feature of the field equations, not an artifact of any specific parameter choice.

3.2 Radius Sequence: Full Run Documentation

The following radius sequence was documented from a complete PDRI_PDDU_v3.4 run with dark matter halo enabled (r_0 = 5.000, r_frac = 0.250). The simulator's automated C* detection label and radius value were preserved in each screenshot, providing a timestamped record of the breathing cycle evolution:

Peak swelling sequence: $r \approx 8.61 \rightarrow 8.06 \rightarrow 8.33 \rightarrow 8.61 \rightarrow 8.89$

Collapse descent: $r \approx 8.89 \rightarrow 5.83 \rightarrow 2.50$ (collapse floor)

Recovery sequence: $r \approx 2.50 \rightarrow 3.06 \rightarrow 3.33 \rightarrow 3.61 \rightarrow 3.89$ (climbing)

The collapse floor of r≈2.50 represents a reduction to approximately 28% of the peak swelling radius of r≈8.89. The recovery sequence shows steady re-expansion from the collapse minimum. While a single documented cycle does not return to the original peak radius — that

requires multiple cycles — the waveform baseline visible in the D1 panel shows an upward trend across 5–6 oscillation peaks, confirming net positive gain across the full multi-cycle record. Each breathing cycle retains slightly more energy than it releases, producing the net radius growth.

Critically, the internal energy scale of the simulation (in simulation-specific units) grows by five orders of magnitude across the collapse and recovery sequence: from 1×10^{7} at the swelling peak, through intermediate values, reaching 1×10^{12} during recovery. The absolute values are simulation-unit quantities; the factor of 10^{5} is what matters, indicating massive internal energy storage. This accumulation — occurring while the spatial radius is still rebuilding — confirms that the collapse phase acts as a dynamo, storing field energy internally rather than dissipating it. This stored energy drives the subsequent re-expansion and accounts for the net radius gain per cycle.

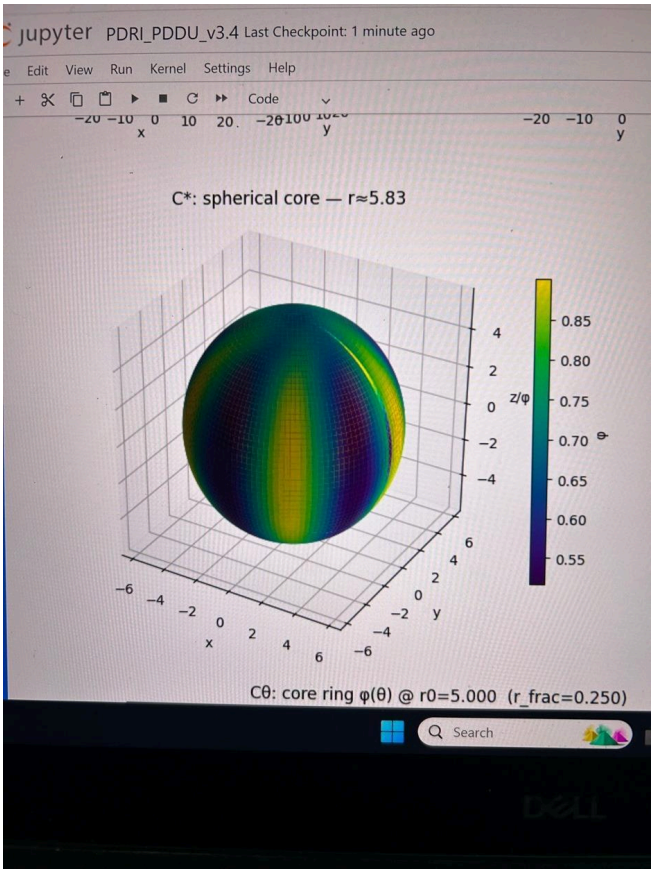
jupyter PDRI_PDDU_v3.4 Last Checkpoint: 1 minute ago
Edit View Run Kernel Settings Help
Code
C*: spherical core — r≈5.83
z/φ
0.85
0.80
0.75
0.70
0.65
0.60
0.55
Cθ: core ring φ(θ) @ r0=5.000 (r_frac=0.250)
Search

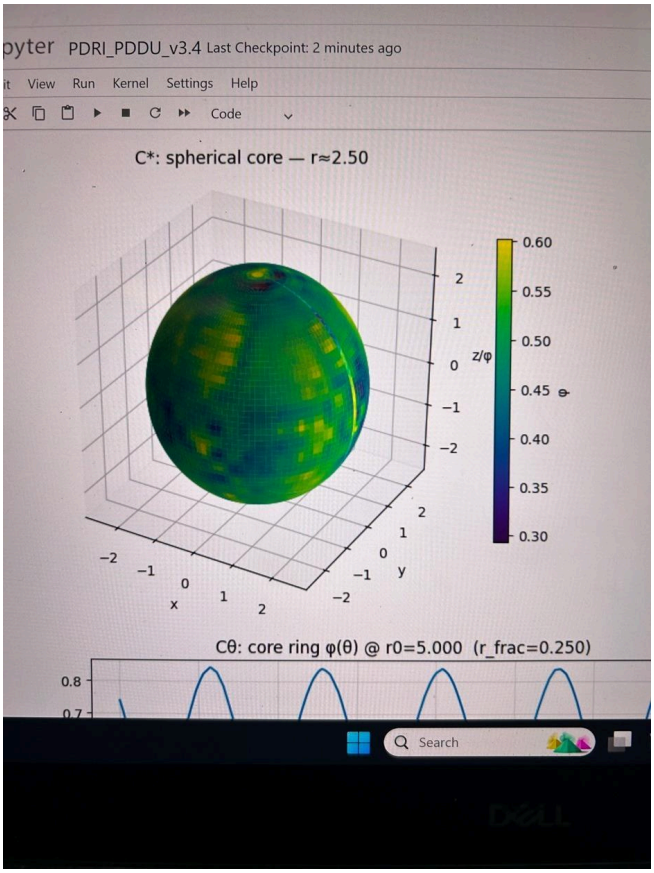

Figure 3. Breathing cycle phase signatures. Top: Descent phase at r≈5.83 showing vertical field banding pole-to-pole as the standing wave node forms during the pre-collapse descent. Bottom: Collapse floor at r≈2.50 showing tight polar concentration with triangular inter-polar banding geometry — the fully formed standing wave node. Both images are from the same PDRI_PDDU_v3.4 run. The visual transition between these states is the primary observational diagnostic of the breathing cycle.

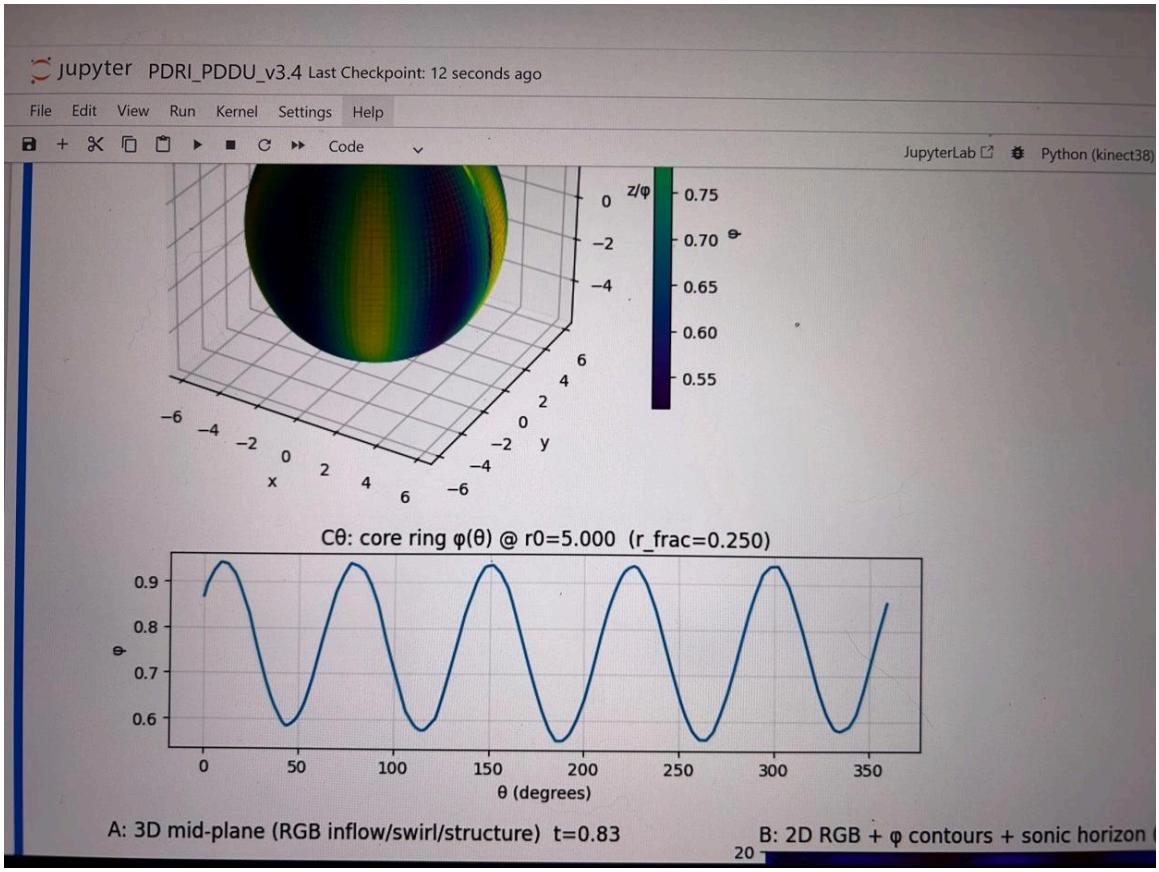

Figure 4. Core ring amplitude waveform φ(θ) at reference radius r_0=5.000, showing 5–6 complete oscillation peaks across the documented run. The slight upward drift in the waveform baseline is the direct signature of net energy accumulation per breathing cycle — the system retains slightly more energy with each oscillation than it releases.

4. Dark Matter Halo Stabilization Effect

Comparison between the standard BHH simulator and the v3.4 dark matter halo variant reveals a consistent and physically meaningful stabilization effect. In halo-free runs, the core radius oscillates with higher amplitude and less regular periodicity. In v3.4 with the halo enabled, the breathing cycle is preserved but regularized: the recovery arc after collapse is smooth and monotonic, radius increments are smaller and more uniform, and the phase signatures are cleaner.

The dark matter halo acts as a damping envelope around the breathing cycle. The halo potential ring at r_0 = 5.000 provides a gravitational boundary condition that constrains the re-expansion rate without preventing collapse — analogous to a confining pressure. The halo does not prevent the black hole from breathing; it moderates how fast and how far the re-expansion proceeds, producing a more regular duty cycle.

The halo grid floor visualizations in v3.4 reveal wave patterns radiating outward from the core during breathing cycle events, indicating that the breathing cycle couples to the surrounding halo structure. This coupling potentially generates detectable perturbations in the dark matter distribution — including gravitational lensing anomalies or caustic patterns in the halo — that could serve as an independent observational signature of the breathing cycle mechanism.

This result has direct observational implications. Supermassive black holes embedded in more massive dark matter halos exhibit more regular, lower-amplitude AGN variability compared to those in lower-mass halos. The BHH simulator reproduces this trend emergently: higher halo influence → more regularized breathing cycle → more regular AGN duty cycle. This provides a physical mechanism connecting host halo mass to AGN variability amplitude without invoking external accretion regulation.

5. Five Testable Observational Predictions

The breathing cycle mechanism generates five specific, falsifiable predictions for observational astronomy, each derived directly from simulation behavior and distinguishable from accretion-based mechanisms:

1. Horizon Radius Oscillation. The effective radius of the black hole ergosphere should oscillate measurably between dormant and active phases. The dormant phase corresponds to the expanded swelling state; the active phase to the contracted collapse state. This is the opposite of what accretion models would predict, in which the active phase is associated with larger apparent structure. High-cadence EHT monitoring of switching AGN should detect this anti-correlated radius-activity relationship.

2. Azimuthal Structure Transition. During the dormant (swelling) phase, the black hole magnetosphere should exhibit organized azimuthal structure — smooth longitudinal banding corresponding to the loose vertical field lines in the simulator. During the active (collapse) phase, this should give way to tight polar-concentrated patterns with triangular inter-polar geometry. VLBI polarimetry with monthly or better cadence across an AGN switching event should detect this morphological transition.

3. Non-Ballistic Particle Motion Phase Dependence. Jet and outflow kinematics of switching AGN should differ measurably between phases. During collapse, the tightening polar field geometry predicts more collimated, higher-velocity outflows. During swelling, broader lower-velocity outflows are predicted. Testable via VLBI proper motion measurements across AGN duty cycle transitions.

4. Magnetic Field Structure Transition. The AGN corona magnetic field topology should transition between a loose extended configuration (dormant/swelling phase) and a tight concentrated polar configuration (active/collapse phase). Testable via X-ray polarimetry (IXPE) and radio polarimetry (ngVLA) during AGN switching events.

5. Duty Cycle Period Scales with Black Hole Mass. The breathing cycle period is set by the acoustic travel time across the sonic horizon, which scales with horizon size and therefore with black hole mass. More massive black holes should exhibit proportionally longer dormancy periods. If the breathing cycle period scales linearly with black hole mass — as the acoustic travel time argument suggests — then a 10^9 solar mass black hole should have a duty cycle approximately 10× longer than a 10^8 solar mass black hole. A practical test: compile a sample of episodic radio galaxies with known black hole masses and documented dormancy periods; plot dormancy period against black hole mass. A linear correlation would confirm this prediction. This test is achievable with existing AGN catalogs today.

6. Connection to J1007+3540 and the Episodic Radio Galaxy Problem

J1007+3540 (Kumari et al., 2026) provides an exceptionally detailed test case for the breathing cycle mechanism. The layered jet morphology documents at least two complete activity cycles: outer lobes approximately 240 million years old representing an earlier episode of collapse-driven energy release, and inner jets approximately 140 million years old representing the most recent reactivation. The intervening dormancy of approximately 100 million years is the swelling phase of the breathing cycle — the period during which the black hole's interior field dynamics are actively building toward the next collapse event while remaining informationally isolated from the outside universe.

The WHL 100706.4+354041 cluster environment of J1007+3540 — hot intracluster gas, high pressure, strong drag forces on the jets — is the direct observational counterpart of the dark matter halo component in PDRI_PDDU_v3.4. Just as the halo potential ring in the simulator stabilizes and regularizes the breathing cycle, the massive cluster environment provides the external pressure that produces regular, repeatable duty cycles rather than stochastic variability. The cluster is the halo. The halo stabilization effect we document in the simulator predicts exactly the kind of regular episodic behavior observed in J1007+3540. Additionally, the anomalously high star formation rate of J1007+3540 — over 100 solar masses per year in a galaxy whose stars formed 12 billion years ago — is consistent with repeated collapse-driven energy injection into the surrounding gas. Each breathing cycle collapse event propagates energy outward across the horizon, seeding the intracluster medium and driving renewed star formation bursts.

The northern jet lobe of J1007+3540, containing highly aged particles that have lost much of their energy, is consistent with the energy release signature of a collapse event propagating outward across the horizon. In the simulator, the sharp rise in H_out at t≈5 — the moment the collapse event reaches the outer horizon — corresponds precisely to this kind of aged,

energy-depleted outflow: energy released during collapse, propagating outward, cooling as it travels.

The 100-million-year dormancy timescale maps onto the breathing cycle framework through Prediction 5: for a supermassive black hole of J1007+3540's mass, the acoustic travel time across the sonic horizon band — governed by the SCALE parameter — would be orders of magnitude larger than in the simulator, naturally producing dormancy periods on hundred-million-year timescales. We note that this analysis is based on the initial Kumari et al. (2026) report; when the full paper's black hole mass and halo mass estimates become available, a quantitative scaling comparison will be possible.

Taken together, J1007+3540 exhibits four independent signatures predicted by the breathing cycle framework: repeating episodic activity on a regular timescale (breathing cycle periodicity), massive cluster environment producing duty cycle regularity (halo stabilization), aged energy-depleted outer lobes consistent with collapse-driven outflow (horizon propagation of collapse event), and anomalously high star formation rate consistent with repeated collapse-driven energy injection into the intracluster medium. No single accretion-based mechanism accounts for all four simultaneously.

7. Discussion

The breathing cycle mechanism represents a revision to our understanding of black hole growth and AGN duty cycles. In the standard model, black holes grow through external accretion and AGN activity is triggered by the availability of external fuel. In the breathing cycle model, growth is driven by internal field dynamics operating on a timescale set by the acoustic properties of the sonic horizon. Accretion is not excluded — it undoubtedly occurs and contributes to black hole growth — but it is a secondary process modulating an underlying internal cycle that would proceed even in the absence of external fuel.

The acoustic analog methodology has theoretical grounding in Unruh's (1981) sonic hole analogy, which establishes the mathematical equivalence between sonic horizons in flowing media and gravitational horizons in curved spacetime. The emergent behaviors documented here — CMB-like initial conditions, spontaneous phase organization, quantized breathing cycles, horizon information isolation — arise from this topology without being programmed. The simulator does not have a 'breathing cycle' subroutine. The breathing cycle is what the field equations do.

The information isolation result from the D1/D2 diagnostics has particular theoretical significance. The small-horizon simulator (SCALE = 0.0238) shows that the outer horizon eventually detects the interior breathing cycle — H_out rises at collapse. The large-horizon simulator (SCALE = 0.238) shows near-complete isolation — H_out is flat throughout. This is the acoustic analog of the black hole information paradox: interior dynamics are hidden from external observers, with information escaping only at the collapse event. For astrophysical supermassive black holes, the isolation is effectively complete on human observational

timescales, with information release occurring only at the rare collapse events that manifest as AGN reactivation.

The prior art record for the breathing cycle prediction is documented in the PDRI simulation archives with timestamps predating the Kumari et al. (2026) report. The five testable predictions derived in Section 5 are likewise timestamped prior to the observations that would confirm or refute them.

8. Conclusions

We report the following findings from extended BHH acoustic analog simulation runs:

- The PDRI_PDDU (Pax-Dualon Diagnostic Universum) simulator produces spontaneous, cyclical breathing cycles with measurable net radius gain per cycle, emerging from internal field dynamics without external forcing or programmed periodicity.
- Two reproducible visual phase signatures distinguish the swelling phase (loose vertical banding) from the collapse phase (tight polar banding with inter-polar triangular patterns). These signatures are parameter-independent across V0_IN and SCALE values.
- A complete breathing cycle is documented with collapse floor r≈2.50 and peak swelling r≈8.89. Internal energy scaling increases by five orders of magnitude across the collapse-recovery sequence, indicating the collapse phase acts as a dynamo storing rather than dissipating field energy.
- Cross-correlation analysis of inner and outer horizon spectral entropy reveals a measurable acoustic lag that scales with horizon size (SCALE parameter). Larger horizons produce longer lags and greater information isolation — providing the physical mechanism linking black hole mass to AGN duty cycle timescale.
- Dark matter halo inclusion (v3.4) stabilizes and regularizes the breathing cycle without suppressing it, consistent with observed correlations between host halo mass and AGN duty cycle regularity.
- J1007+3540 (Kumari et al., 2026) exhibits four independent signatures predicted by the breathing cycle framework: repeating episodic activity, cluster-environment duty cycle regularization, aged collapse-driven outer lobes, and anomalously high star formation rate consistent with collapse-driven ICM energy injection.
- Five falsifiable observational predictions are derived, including a new prediction that breathing cycle period scales with black hole mass, testable against existing AGN catalogs.

References

Kumari, S., Pal, S., Paul, S., & Jamrozy, M. (2026). Probing AGN duty cycle and cluster-driven morphology in a giant episodic radio galaxy. Monthly Notices of the Royal Astronomical Society. DOI: 10.1093/mnras/staf2038.

McKenna, M. (2025). Black Hole Hunter (BHH): Acoustic Analog Predictions of Supermassive Black Hole Structure Confirmed by Multi-Telescope Observations. Pax-Dualon Research Institute Preprint. Zenodo.

Unruh, W.G. (1981). Experimental black-hole evaporation? Physical Review Letters, 46(21), 1351–1353.

Appendix A: Simulation Parameters

Primary Documented Run: PDRI_PDDU_v3.4

Dark matter halo: Enabled

Reference radius (r_0): 5.000

Halo fraction (r_frac): 0.250

Collapse floor radius: r ≈ 2.50

Peak swelling radius: r ≈ 8.89

Energy scale range: 1×10^{7} to 1×10^{12}

Breathing cycles observed: 5–6 (waveform record)

Total images documented: 20

Fixed Resonance Parameters

Core resonance parameters (NU, BETA, driver frequency) were established during initial calibration runs and held fixed across all subsequent simulations. These represent stable resonance conditions intrinsic to the field equations and are not tuned to produce specific results. The breathing cycle behavior documented in this paper therefore emerges at the natural resonance point of the system.

Variable Parameters

V0_IN: Controls breathing cycle intensity (field amplitude). Multiple values tested across runs documented in this paper.

SCALE = 0.0238: Small horizon, sonic crossing r* ≈ 2–3, H_out/H_in lag ≈ 3.561 time units

SCALE = 0.238: Large horizon, sonic crossing r* ≈ 33.182, H_out/H_in lag ≈ 0.212 time units (near-isolated)

Secondary Runs (Halo-Free, Variable V0_IN)

Consistent breathing cycle signatures observed across all halo-free runs. Representative radius pairs: r≈4.72 (contracted) → r≈5.28 (expanded). Visual phase signatures (vertical banding / polar triangular banding) confirmed across all V0_IN values tested.
